

Deposition of Thin Films Composed of $\text{Fe}_{81}\text{B}_{13.5}\text{Si}_{3.5}\text{Co}_2$ Material by PLD Method Using the ArF Excimer Laser

Waldemar MRÓZ*¹, Artur PROKOPIUK*¹, Michael L. KORWIN-PAWLOWSKI*² and Sylwia BURDYŃSKA*¹

^{*1} *Military University of Technology, Institute of Optoelectronics
ul. Kaliskiego 2, 00-908 Warsaw, Poland
E-mail : wmroz@wat.edu.pl*

^{*2} *Université du Québec en Outaouais, Département d'informatique et d'ingénierie,
101, rue Saint-Jean-Bosco, Gatineau (Québec), J8X 3X7 Canada*

Depositions of thin films, composed of $\text{Fe}_{81}\text{B}_{13.5}\text{Si}_{3.5}\text{Co}_2$ material were performed with ArF excimer laser ($\lambda = 193$ nm). The material, with expected large magnetoelastic coefficient is potentially applicable in sensor and actuator technology. Depositions were done on polished $\langle 100 \rangle$ orientation Si substrates held at different temperatures: RT, 250°C, 450°C and 550°C. Results of AFM, MFM, SEM, EDS and FTIR measurements of the layers as a function of process parameters, in particular of the substrate temperature, are presented.

Keywords: magnetic materials, magnetic field sensors, pulsed laser deposition

1. Introduction

Increased interest in recent years has been paid to electromagnetic field sensors and in particular to photonic, and more narrowly, fiber optic sensors for those applications [1-5]. A review of electromagnetic field photonic sensors is provided in [6]. Some of those sensors are based on the magnetostrictive effect with the material used in form of ceramic jackets inducing longitudinal strain in an optical fiber [4] or magnetic shape memory alloys bonded to fiber Bragg gratings [5]. The relatively low sensitivity of simple nickel and cobalt as magnetostrictive coatings for optical fibers [1] could be significantly improved by use of more complex materials such as magnetic metallic glasses [7]. The composition of $\text{Fe}_{81}\text{Si}_{3.5}\text{B}_{13.5}\text{C}_2$ (with iron, silicon, boron, carbon) known commercially as METGLAS[®]2605SC is one to which attention of researchers was drawn, due to its excellent magnetostrictive properties when deposited by magnetron sputtering [8, 9]. Cobalt-doped nickel ferrite thin films applied by dip-coating technique [10] and nickel zinc ferrite thin films applied by sol-gel technique [11] have also been used on optical fibers for sensing purposes.

It is well known that pulse laser deposition (PLD or laser ablation) shows specific advantages over other methods of depositions of thin films, such as evaporation or sputtering. PLD maintains better in the deposited films the stoichiometric composition of the source, and also allows a very good control of the thickness of the deposited films and their uniformity. These parameters are important for reproducible fabrication and to achieve good properties of fiber optic sensors.

There is a need to develop improved materials using well established low-cost manufacturing techniques to be used as PLD deposition targets in thin films fabrication, in particular for fiber optic sensors of magnetic fields. We have identified the $\text{Fe}_{81}\text{B}_{13.5}\text{Si}_{3.5}\text{Co}_2$ composition as a potentially interesting material for this application. In this

paper we are presenting results of optimization of the PLD process to achieve a fine nanocrystalline structure of deposited films, which is advantageous for use as magnetostrictive films on fiber optic magnetic field sensors.

2. Experimental

$\text{Fe}_{81}\text{B}_{13.5}\text{Si}_{3.5}\text{Co}_2$ (with iron, boron, silicon, cobalt at atomic % indicated in subscripts) as hot pressed targets with guaranteed 99.9% purity were supplied by Goodfellow Cambridge Ltd. of Huntingdon, England. The target dimensions were 35 x 45 x 10 mm +/- 0.5 mm. As deposition substrates we used pieces of $\langle 100 \rangle$ orientation polished silicon wafers.

The films were deposited using a computer-controlled target-substrate mechanism PLD system with a turbomolecular oil-free pump capable of achieving a 10^{-6} mbar residual pressure in the vacuum chamber. A Neocera radiant substrate heater with a maximum achievable temperature of 950°C was used to facilitate the nanocrystallization of deposited layers. The target to substrate distance was 6 cm. An ENI Co. RF plasma generator was used for in-situ substrate cleaning, which improves its chemical reactivity and accelerates the interface chemical reactions. An ex-situ Veeco MultiMode AFM Nanoscope was used in the Tapping Mode[™] and in PhaseImaging[™] modes, allowing us to obtain material phase contrast maps for the investigated surfaces and a concurrent analysis of the material's morphology. In our experiments we were using a Lambda Physics LPX 305i ArF excimer laser with the following rated output parameters: wavelength $\lambda = 193$ nm, maximum energy per pulse 0.7 J, pulse width 15 to 20 ns, and repetition rate up to 50 Hz. The PLD system was equipped with several optical control instruments, namely a spectrograph, optical microscopes for substrate observation and a Thomson parabola ion spectrometer for ion beam diagnostics. Ex-situ we have used a Hitachi S3000N SEM with an Electron Dispersive X-ray Spectroscopy (EDS) probe for analysis of

the atomic composition of the deposited films and a Perkin-Elmer Fourier Transform Infrared (FTIR) spectrometer.

3. Results and discussion

We have performed a number of deposition runs in different conditions to zero in on the desired process. Those conditions are listed in Table 1.

Table 1 PLD process parameters

Run No.	Nominal thickness	Number of laser shots	Laser repetition rate	Substrate temperature
1	1500 nm	45000	5 Hz	R.T
2	2000 nm	60000	10 Hz	250°C
3	50 nm	1500	5 Hz	450°C
4	200 nm	6000	10 Hz	450°C
4	2000 nm	60000	10 Hz	450°C
6	2000 nm	60000	10 Hz	550°C

Each process run consisted of two samples. The chamber background pressure was lower than 10^{-5} mbar, the laser energy on the target was 300 mJ, which corresponds to a fluence of 7 J/cm^2 and the substrate temperatures T_s were varied from room temperature (R.T.) to 550°C in 4 steps by using the system's heater, in order to investigate the effect of substrate temperature on the growth and crystallization of the layers and on the formation on their surface of three-dimensional structures. The temperatures were measured with a thermocouple at the substrate with an accuracy of $\pm 50^\circ\text{C}$; they were a few hundred degrees lower than the heater controller setting temperatures due to an alumina shield used before the heater to isolate the heater from contamination by the deposition material. The nominal thickness was determined from test runs calibrated by profilometric measurements; it is accurate $\pm 20\%$.

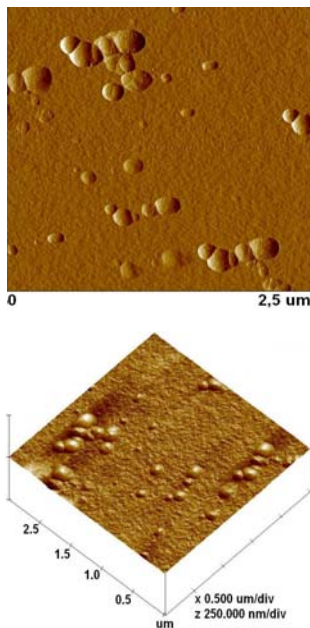


Fig. 1 Topography of layers deposited at $T_s=20^\circ\text{C}$ with the laser frequency $f=5 \text{ Hz}$

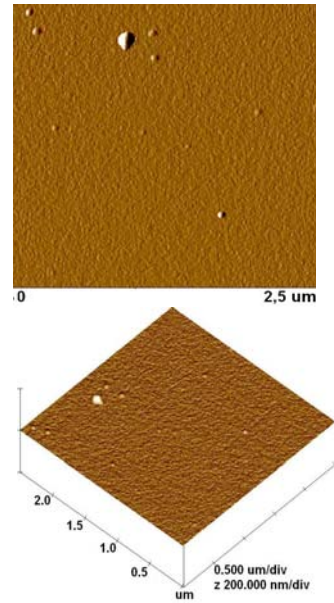


Fig. 2 Topography of layers deposited at $T_s=250^\circ\text{C}$ with the laser frequency $f=10 \text{ Hz}$

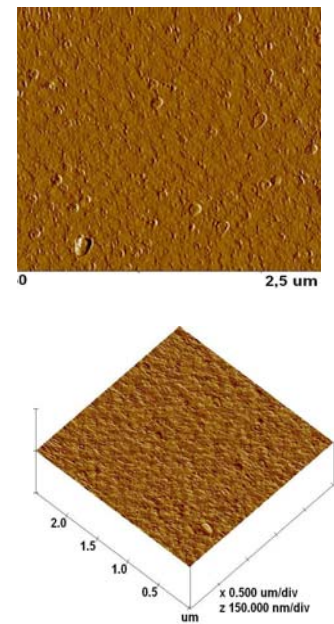


Fig. 3 Topography of layers deposited at $T_s=450^\circ\text{C}$ with the laser frequency $f=10 \text{ Hz}$

Examples of AFM imaging of the surfaces of the layers deposited at different temperatures are given in Figs. 1 to 4. Already on the surface of samples deposited at $T_s=R.T.$ one can observe a large quantity of three-dimensional hillock structures. At the $T_s=250^\circ\text{C}$ deposition the surface of the layers is smoother and the number of hillocks formed is clearly smaller (Fig. 2). At both R.T. and 250°C substrate temperatures the layers seem amorphous, except for the hillocks. Phase maps of layers formed at $T_s=450^\circ\text{C}$ are not as uniform as at the lower temperatures. The images showed two colors, which may indicate the start of recrystallization of the material. At $T_s=550^\circ\text{C}$ the

recrystallization process is intensified, as evidenced by a fine nanocrystalline structures with clear oval-shaped grain boundaries. The grains are oriented in one direction, which may have consequences in the orientation of the magnetic domains.

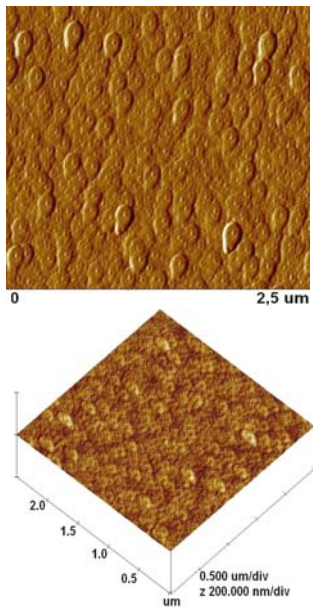


Fig. 4 Topography of layers deposited at $T_s=550^\circ\text{C}$ with the laser frequency $f=10\text{Hz}$

characteristic for the type of deposited material and the process, which is typical for particulates generated by PLD [12]. Further analysing the AFM phase images, we notice that the hillocks are made up of a large quantity of nanometric size grains. The grain boundaries in the structure obtained at 550°C are not as sharp as those at lower temperatures because the layers have recrystallized. As expected, in the investigated range of substrate temperature, 550°C shows the highest degree of recrystallization of the layers.

We have looked at layers of different thicknesses: 50 nm, 200 nm and 2000 nm formed at the substrate held at 450°C . The surface structures seemed very similar for all thicknesses, with a nanocrystalline grainy structure most prominent on the 2000 nm layers.

In the course of AFM studies of the layers we have obtained data on the surface roughness for the 2000 nm thick layers (except the $T_s=R.T.$ layer which was 1500 nm thick) as a function of substrate temperature (Table 2) and for the hillocks themselves (Table 3.) Shown in the tables are average R_a , root-mean-square R_{ms} and maximum R_{max} roughness. The roughness figures for the layer were taken over a $2.5\mu\text{m}$ square area. They do not vary very much for the elevated T_s layers, but the roughness of layers deposited at room temperature substrates is much higher. For comparison, the roughness of the silicon substrate prior to deposition was measured as 0.2 nm. The heights of the hillocks are in the range of about 80 to 200 nm.

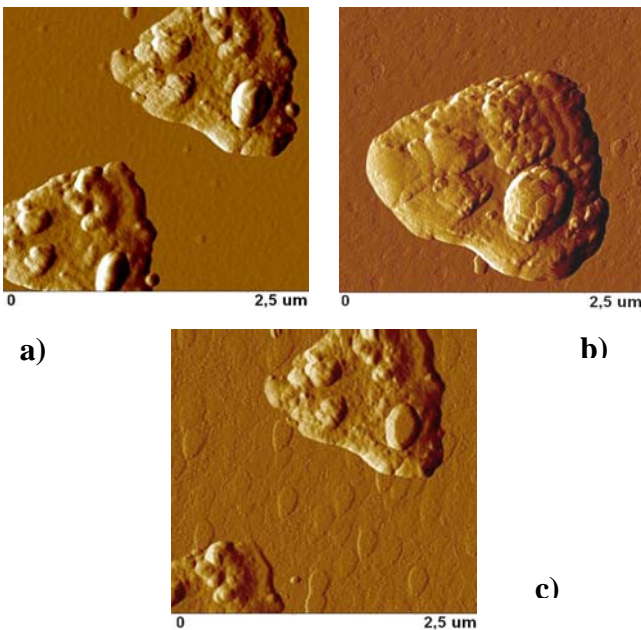


Fig. 5 Images of structural elements on the surfaces of layers deposited at different substrate temperatures: a) 250°C , b) 450°C , c) 550°C

Fig. 5 provides AFM images of the hillock structures which formed on the surface of the layers. The hillocks are very similar in their triangular shapes, notwithstanding the $\langle 100 \rangle$ orientation of the silicon, and have dimensions of a few micrometers and grainy structures regardless of the substrate temperatures. Therefore, the structures are

Table 2 AFM roughness of the layers

Roughness	@ $T_s=R.T.$	250°C	450°C	550°C
R_a	1.83 nm	0.25 nm	0.45 nm	0.93 nm
R_{ms}	3.46 nm	0.79 nm	0.65 nm	1.20 nm
R_{max}	43.3 nm	29.4 nm	13 nm	10.3 nm

Table 3 AFM roughness of the hillocks

Roughness	@ $T_s=250^\circ\text{C}$	450°C	550°C
R_a	11.6 nm	15.7 nm	7.3 nm
R_{ms}	15.8 nm	24.2 nm	10.8 nm
R_{max}	136 nm	201 nm	86 nm

In continuation of our study we have analysed the chemical composition of the layers using an EDS probe on the SEM. In this method the investigated material is bombarded by electrons. A detector converts the X-rays emitted by the elements present in the material into electronic pulses with a resolution of at least 130 eV. This allows determining the concentrations of elements down to 0.5%, but does not easily distinguish between elements showing response closer to each other than the resolution of the system. This has an important bearing on our measurements since the iron (Fe) and cobalt (Co) pulses and also boron (B) and carbon (C) pulses are very close.

On Fig. 6 is shown an example of the EDS response spectrum for a 2000 nm layer deposited on a substrate held

at 250°C. The overlap of the Fe and Co peaks in the range from 0.68 to 0.85 keV and B and C peaks in the range from 0.18 to 0.28 keV is well illustrated.

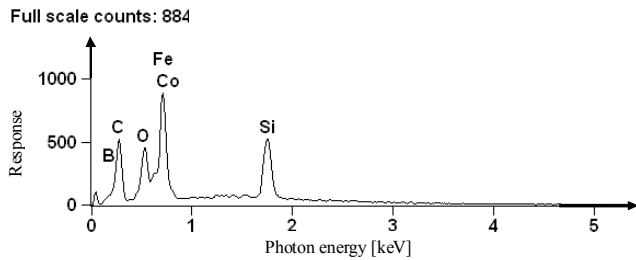


Fig. 6 EDS response for a 2000 nm layer deposited at $T_s=250^\circ\text{C}$

In Table 4 are given results of analysis the composition in atomic percentages of 2000 nm layers deposited at 250°C. For the T_s at 250°C and 450°C the layers compositions were closest to the composition attested by the manufacturer of the target material.

Table 4 EDS atomic composition

Element	Fe	B	Si	Co
Composition				
Deposited layer	83%	8.5%	3.5%	5.0%
Target mater.	81%	13.5%	3.5%	2.0%

The figures given in Table 4 have been adjusted by eliminating residual carbon content, which most likely came from the oil diffusion pump of the measuring system and oxygen content which was most likely due to oxidation of the layers. The accuracy of EDS is not greater than 0.5%. It must be noted that the material oxidizes quite easily when stored in air absorbing from 5% up to about 20% of oxygen after prolonged storage in air. Therefore, all measurements presented in this paper were made directly after the deposition. For practical application the material will have to be protected by passivating layers, for example by thin films of chromium or gold.

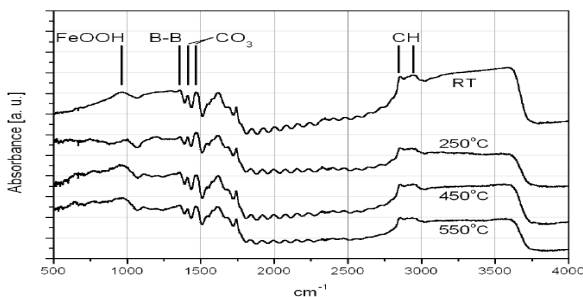


Fig. 7 FTIR absorption spectra in arbitrary units for layers deposited on substrates at different T_s

The FTIR spectra on Fig. 7 have been shifted along the y-axis for clarity. The FeOOH peak about 960 cm^{-1} significantly increases at $T_s=450^\circ\text{C}$ compared with $T_s=250^\circ\text{C}$ and holds its value at 550°C. The boron B-B bonds peak at 1360 cm^{-1} remains steady at all temperatures.

The carbon peaks CO_3 (at 1410 cm^{-1} and 1460 cm^{-1}) and C-H (2850 cm^{-1} and 2950 cm^{-1}) are most likely due to source contamination by CO_2 in the atmosphere, while the OH bonds at 1600 cm^{-1} and in the range from 3000 to 3600 cm^{-1} represent water absorption in the sample. They are higher at R.T. than at higher temperatures, where water desorbs easier.

4. Conclusions

The deposition conditions of $\text{Fe}_{81}\text{B}_{13.5}\text{Si}_{3.5}\text{Co}_2$ material by PLD method using the ArF excimer laser have been investigated and the results analysed in terms of observed surface morphology properties of the layers using AFM, SEM, and their atomic composition using EDS and FTIR. We have established that nanocrystallisation of the layers clearly occurred at the substrate temperature of 450°C and 550°C, while layers deposited on substrates held at room temperature showed an amorphous character. The layers oxidize readily when stored in air and protective layers would have to be used to prevent oxidation in practical applications. On the other hand, the surface reactivity of the layers may lead to applications where their magnetoelastic properties are modified by the presence of chemicals in the surrounding atmosphere. We are planning to extend this study to include the magnetic and magnetoelastic properties of the layers and to investigate the potential applications in electromagnetic field sensors and energy harvesting devices.

Acknowledgements

This work was supported by Canadian NSERC (Discovery) and CFI grants and by the grant No. T00C 004 29 from the Polish State Committee for Scientific Research.

References

- [1] A. Yariv, and H. V. Winsor: Opt. Lett. 5 (1980) 87
- [2] K.-S. Lee, Yu S. Lee and Su J. Suh: Proc. SPIE 2292 (1994) 2292-07
- [3] S. Rengarajan and R. M. Walser: J. Appl. Phys, 81, (1997) 4278
- [4] M. Sedlar, V. Matejec and I. Paulicka: Sensors and Actuators 84, (2000) 29
- [5] C. Ambrosino, P. Capoluongo, S. Campopiano, A. Cutolo, A. Cusano, M. Giordano, D. Davino and C. Visone: Proc. SPIE, 5952, (2005) 595217
- [6] V. M. N. Passaro, F. Dell’Olio and F. De Leonadis: Progr. Quant. Electron, 30, (2006) 45
- [7] A. D. Kersey, D. A. Jackson and M. Corke: J. Lightwave Technol. LT-3, (1984) 836
- [8] B. Kundys, Yu. Bukhantsev, H. Szymczak, M.R.J. Gibbs and R. Żuberek: J. Magnetism and Magn. Mat. 258-259, (2003) 551
- [9] B. Kundys, Yu. Bukhantsev, H. Szymczak, M.R.J. Gibbs and R. Żuberek: J. Phys. D: Appl. Phys. 35 (2002) 1095
- [10] M. Sedlar and L. Pust: Ceramics International 21, (1995) 21
- [11] M. Sedlár, V. Matejčec, T. Grygar and J. Kadlecová: Ceramics International 26, (2000) 507
- [12] Li-Chyong Chen in “Pulsed Laser Deposition of Thin Films” ed. by Douglas B. Chrisey and Graham K. Hubler (John Wiley and Sons, Inc., New York, 1994) p. 167

(Received: June 16, 2008, Accepted: November 25, 2008)